



HAL
open science

Synthesis, in silico study, and biological evaluation of cyclosulfamide derivatives as new anticholinesterase inhibitors

Abdeslem Bouzina, Abdelhak Djemel, Omar Sekiou, Imededdine Kadi, Yousra Ouafa Bouone, Rachida Mansouri, Zineb Aouf, Malika Ibrahim-Ouali, Nour Eddine Aouf

► To cite this version:

Abdeslem Bouzina, Abdelhak Djemel, Omar Sekiou, Imededdine Kadi, Yousra Ouafa Bouone, et al.. Synthesis, in silico study, and biological evaluation of cyclosulfamide derivatives as new anticholinesterase inhibitors. *Journal of Molecular Structure*, 2023, pp.135527. 10.1016/j.molstruc.2023.135527 . hal-04063526

HAL Id: hal-04063526

<https://amu.hal.science/hal-04063526>

Submitted on 9 Apr 2023

HAL is a multi-disciplinary open access archive for the deposit and dissemination of scientific research documents, whether they are published or not. The documents may come from teaching and research institutions in France or abroad, or from public or private research centers.

L'archive ouverte pluridisciplinaire **HAL**, est destinée au dépôt et à la diffusion de documents scientifiques de niveau recherche, publiés ou non, émanant des établissements d'enseignement et de recherche français ou étrangers, des laboratoires publics ou privés.

Synthesis, *in silico* study, and biological evaluation of cyclosulfamide derivatives as new anticholinesterase inhibitors

Abdeslem Bouzina^{a*}, Abdelhak Djemel^b, Omar Sekiou^c, Imededdine Kadi^b, Youssa Ouafa Bouone^a, Rachida Mansouri^c, Zineb Aouf^a, Malika Ibrahim-Ouali^d, Nour Eddine Aouf^a

^aLaboratory of Applied Organic Chemistry, Bioorganic Chemistry Group, Department of Chemistry, Sciences Faculty, Badji-Mokhtar-Annaba University, Box 12, 23000 Annaba, Algeria.

^bResearch Unit in Medicinal Plants, URPM, 3000 Laghouat, attached to Research Center of Biotechnology, CRBt, 25000 Constantine, Algeria.

^cEnvironmental Research Center (CRE), 23000 Annaba, Algeria.

^dAix Marseille Univ, CNRS, Centrale Marseille, iSm2, F-13397 Marseille, France.

*Corresponding author. Email: abdeslem.bouzina@univ-annaba.dz ; bouzinaabdeslem@yahoo.fr

Abbreviations list

AD: Alzheimer's disease

AChE: Acetylcholinesterase

BuChE: Butyrylcholinesterase

ACh: Acetylcholine

CNS: Central Nervous System

FDA: The U.S. Food and Drug Administration

MD: Molecular dynamic

Abstract

After the great spread of Alzheimer's disease (AD) in the past few years, many researchers directed their work toward developing an effective treatment for this disease and to discovering very advanced drugs. Cyclosulfamides are considered **as** versatile pharmacophores in the construction of new molecules with excellent activities. Therefore, a series of cyclosulfamide have been synthesized and evaluated as anti-Alzheimer agents through *in vitro* acetylcholinesterase (AChE) and butyrylcholinesterase (**BuChE**) inhibition. Most of tested compounds showed an average inhibitory activity against two targeted enzymes compared with the reference ligand. Specifically, **10a** **showed** the best inhibition of AChE enzyme with an

IC₅₀=45.30±0.88μM; while **4a** exhibited the most potent BuChE enzyme inhibition with an IC₅₀=52.87±3.73μM.

Further, we were able to determine a feasible binding mode for cyclosulfamide derivatives owing to molecular docking studies, which offered prospective evidence to identify significant interactions between the active site of AChE and the synthesized ligands.

Following the encouraging findings of the molecular docking investigation, the complex **AChE-10a** was put through a 100ns Desmond of Schrodinger simulation of molecular dynamics (MD), during which the receptor-ligand combination showed significant stability after 10 ns of MD simulation.

Keywords: Cyclosulfamides, Anticholinesterase inhibition, Molecular docking study, MD simulation.

1. Introduction

Neurodegenerative diseases such as Alzheimer, Parkinson and Epilepsy are chronic disorders affecting the nervous system progressively. Alzheimer disease (AD) is one of the greatest challenges in medical practice inducing significant socioeconomic impacts. It is frequently reported in old people and the number of affected persons actually might triplicate by 2050 (1 for 85) [1]. Patients suffering from AD showed several symptoms, particularly memory decreasing and cognitive disorders [2]. These neurologic dysfunctions are a result of cholinergic deficits in different brain parts, due to the alteration of cholinergic neurons [3]. AChE and BuChE are mainly enzymes that modulate the acetylcholine neurotransmitter levels in different neurologic conditions [4]. Consequently, the inhibition of dual AChE and BuChE is considered as a potent strategy to attenuate symptoms and the worsening of AD, and many other neuromuscular disruptions [1,5]. Until the day; few drugs approved by FDA were used in the clinical treatment of AD: aducanumab, galantamine, rivastigmine, donepezil, and tacrine which has been withdrawn from the market. However, their hepatotoxicity and gastrointestinal disorders were reported [6]. Therefore, the development of a new drug or molecule candidate for the treatment of AD has become a necessity.

Heterocyclic scaffolds present a considerable importance in medicinal chemistry constituting the building block of a remarkable number of biologically active entities including many commercialized drugs [7]. Cyclosulfamides are a specific class of heterocycles that incorporate the well-known pharmacophore (N-SO₂-N). The capacity of such compounds to exhibit beneficial pharmacological activities was widely reported in the literature, indeed sulfamide-based heterocyclic compounds showed antibacterial [8], antiviral [9], and anticancer activities

[10]. Cyclosulfamides were also investigated for their inhibitory effects against a great number of enzymes [11]. For example, compound **1** showed inhibition against 11 β -hydroxysteroid dehydrogenase 1 inhibitor (11 β -HSD1) for the potential treatment of ischemic brain injury [12]. Compounds **2** and **3** were evaluated as inhibitors of aspartic proteases of types HIV-1 protease and γ -secretase respectively [13,14]; the inhibition of γ -secretase is known to be efficient in preventing the progression of AD [15]. Inhibitory activity against serine protease of type human leukocyte elastase (HLE) was found in analogues of compound **4** [11], this activity can result in an anti-inflammatory effect [16]. Many other cyclosulfamide-based molecules were described as inhibitors of Protein Tyrosine Phosphatase (PTP) [17], HIV-1 non-nucleoside reverse transcriptase [18], cholesteryl ester transfer protein (CETP) [19], and noroviruses [20].

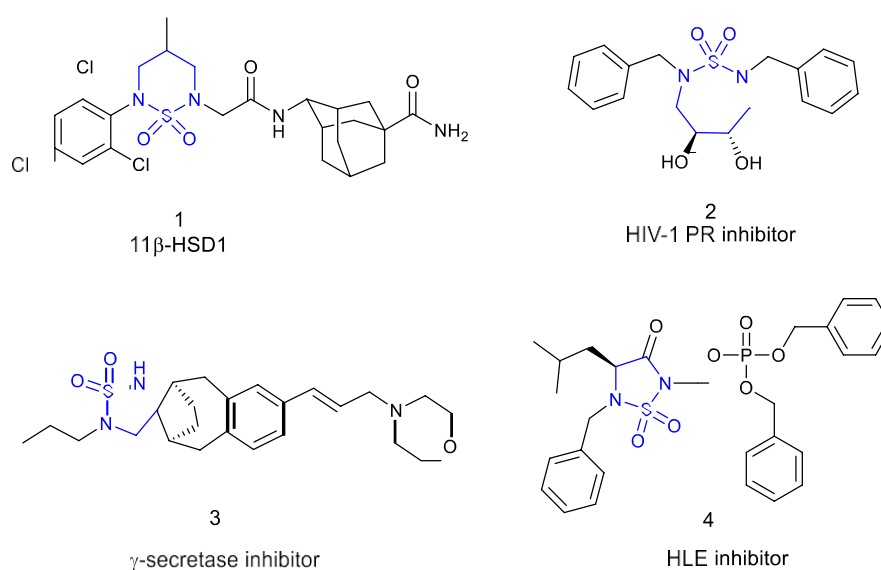


Figure 1. Structures of some biologically active cyclosulfamides.

The main focus of this study is to evaluate derivatives of cyclosulfamide for the first time as AChE and BuChE inhibitors, in order to reduce the neurologic disorders and improve the neurotransmission state in AD patients. Additionally, *in-silico* investigations against AChE were also performed to verify the anti-alzheimer activities.

The design strategy of this study is described in Figure 2.

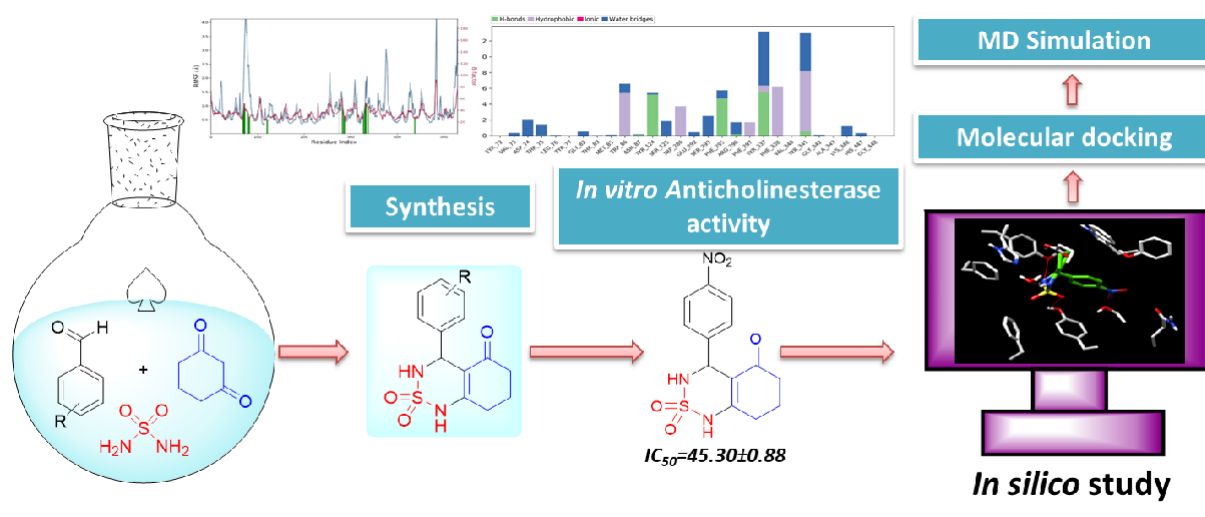


Figure 2. Schematic representation of the design strategy illustration.

2. Material and methods

2.1. Chemistry

2.1.1. Chemical methods

All chemicals and solvents were purchased from common commercial sources (Sigma Aldrich) and were used as received without any further purification. All reactions were monitored by TLC on silica Merck 60 F₂₅₄ percolated aluminum plates and were developed by spraying with ninhydrin solution. Proton nuclear magnetic resonance (¹H NMR) spectra were recorded on a Brücker spectrometer at 400 MHz. Chemical shifts are reported in δ units (ppm) with TMS as reference (δ 0.00). All coupling constants (*J*) are reported in Hertz. Multiplicity is indicated by one or more of the following: s (singlet), brs (broad singlet), d (doublet), dd (doublet of doublet), t (triplet), td (triplet of doublet), q (quartet), m (multiplet). Carbon nuclear magnetic resonance (¹³C NMR) spectra were recorded on a Brücker at 100 MHz. Chemical shifts are reported in δ units (ppm) relative to DMSO-*d*₆ (δ 39.52). Infrared spectra were recorded on a Perkin Elmer 600 spectrometer. The purity of the final compounds (greater than 95%) was determined by uHPLC/MS on an Agilent 1290 system using a Agilent 1290 Infinity ZORBAX Eclipse Plus C18 column (2.1 mm × 50 mm, 1.8 μm particle size) with a gradient mobile phase of H₂O/CH₃CN (90:10, v/v) with 0.1% of formic acid to H₂O/CH₃CN (10:90, v/v) with 0.1% of formic acid at a flow rate of 0.5 mL/min, with UV monitoring at the wavelength of 254 nm with a run time of 10 min. Microanalysis spectra were performed by Elementar Analyzer (Euro E.A. 3000-V3.0-single-2007) and the determined values were within the acceptable limits of the calculated values. Melting points were recorded on a Büchi B-545 apparatus in open capillary

tubes. Microwave assisted reactions were carried out using a Biotage Initiator Microwave Synthesizer 2.0 with a nominal power of 400 W. The reactions were carried out in a reactor to M.W (volume: 10 mL) under pressure at room temperature.

2.1.2. Typical experimental procedure for the synthesis of benzothiadiazinone dioxide

In a reactor MW (volume: 10 mL) taken a mixture of aldehyde (1 mmol), sulfamide (1 mmol), and cyclohexane-1,3-dione (1 mmol) in the presence of H₂SO₄ (0.1 mmol)/CH₃COOH (0.9 mmol) as catalyst under solvent-free at room temperature. The reaction mixture was subjected to microwave irradiation for appropriate time. After completion of the reaction (5-10 min), as indicated by TLC, silica gel; dichloromethane:methanol (9:1), mixture of ethanol and acetone (9:1) or mixture of ethyl acetate and n-hexane (5/5) was added to the reaction mixture and pure product was crystallized to 6 °C overnight. The products were finally filtered and dried.

4-phenyl-4,6,7,8-tetrahydro-1H-benzo[c][1,2,6]thiadiazin 5(3H) -one 2,2-dioxide (1a, C₁₃H₁₄N₂O₃S):

Crystal; 92 % yield; R_f = 0.20 (CH₂Cl₂/CH₃OH:85/15); ¹H NMR (400 MHz, DMSO-d₆): δ = 1.95-2.02 (m, 2H, CH₂), 2.20-2.29 (m, 1H, CH₂), 2.38-2.43 (m, 1H, CH₂), 2.43-2.50 (m, 2H, CH₂), 5.35 (d, J = 6.0 Hz, 1H, CH*), 7.20-7.24 (m, 5H, H-Ar), 7.93 (d, J = 4.4 Hz, 1H, NH-CH*), 10.84 (br s, 1H, NH) ppm; ¹³C NMR (100 MHz, DMSO-d₆): δ = 22.98, 27.55, 36.99, 55.69, 107.90, 126.78, 127.45, 127.81, 139.36, 156.00, 194.42 ppm; IR (KBr): ν = 3286 (NH), 3121 (NH), 1632 (C=O), 1598 (C=C), 1356 and 1171 (SO₂) cm⁻¹; MS: (m/z) = 279.0 (M+1); Anal. Calc. for C₁₃H₁₄N₂O₃S: C, 56.10; H, 5.07; N, 10.07; Found: C, 56.13; H, 5.02; N, 10.03.

4-(2-fluorophenyl)-4,6,7,8-tetrahydro-1Hbenzo[c][1,2,6]thiadiazin-5(3H)-one 2,2-dioxide (2a, C₁₃H₁₃FN₂O₃S):

White powder; 91 % yield; R_f = 0.19 (CH₂Cl₂/CH₃OH:85/15); ¹H NMR (400 MHz, DMSO-d₆): δ = 1.93-2.05 (m, 2H, CH₂), 2.21-2.29 (m, 1H, CH₂), 2.30-2.40 (m, 1H, CH₂), 2.52-2.65 (m, 2H, CH₂), 5.60 (d, J = 8.0 Hz, 1H, CH*), 7.02 (t, J = 8.0 Hz, 1H, H-Ar_{ortho}), 7.13 (t, J = 12.0 Hz, 2H, H-Ar_{para, meta}), 7.27 (q, J = 8.1 Hz, 1H, H-Ar_{meta}), 8.01 (d, J = 8.0 Hz, 1H, NH-CH*), 10.91 (br s, 1H, NH) ppm; ¹³C NMR (100 MHz, DMSO-d₆): δ = 20.75, 27.83, 36.30, 49.75, 106.45, 115.13, 113.11, 126.31, 129.04, 129.65, 158.78, 164.73, 195.92 ppm; IR (KBr): ν = 3261 (NH), 3108 (NH), 1606 (C=O),

1488 (C=C), 1353 and 1171 (SO₂) cm⁻¹; MS: (m/z) = 297.1 (M+1); Anal. Calc. for C₁₃H₁₃FN₂O₃S: C, 52.69; H, 4.42; N, 9.45; Found: C, 52.60; H, 4.37; N, 9.49.

4-(3-fluorophenyl)-4,6,7,8-tetrahydro-1H-benzo[c][1,2,6]thiadiazin-5(3H)-one 2,2-dioxide
(**3a**, C₁₃H₁₃FN₂O₃S):

White powder; 92 % yield; R_f = 0.18 (CH₂Cl₂/CH₃OH:85/15); ¹H NMR (400 MHz, DMSO-d₆): δ = 1.92-2.03 (m, 2H, CH₂), 2.21-2.27 (m, 1H, CH₂), 2.29-2.38 (m, 1H, CH₂), 2.50-2.57 (m, 2H, CH₂), 5.59 (d, J = 7.01 Hz, 1H, CH*), 7.02 (td, J₁ = 7.60, J₂ = 1.0 Hz, 1H, H-Ar_{meta}), 7.02-7.22 (m, 2H, H-Ar_{ortho, para}), 7.28 (ddd, J₁ = 15.2, J₂ = 5.4, J₃ = 1.8 Hz, 1H, H-Ar_{meta}), 8.05 (d, J = 7.20 Hz, 1H, NH-CH*), 10.98 (br s, 1H, NH) ppm; ¹³C NMR (100 MHz, DMSO-d₆): δ = 20.99, 28.05, 38.60, 49.96, 106.66, 114.93, 123.33, 126.53, 129.29, 129.99, 158.94, 161.46, 196.19 ppm; IR (KBr): ν = 3429 (NH), 3268 (NH), 1632 (C=O), 1606 (C=C), 1340 and 1168 (SO₂) cm⁻¹; MS: (m/z) = 297.0 (M+1); Anal. Calc. for C₁₃H₁₃FN₂O₃S: C, 52.69; H, 4.42; N, 9.45; Found: C, 52.64; H, 4.48; N, 9.52.

4-(4-fluorophenyl)-4,6,7,8-tetrahydro-1H-benzo[c][1,2,6]thiadiazin-5(3H)-one 2,2-dioxide
(**4a**, C₁₃H₁₃FN₂O₃S):

White powder; 90 % yield; R_f = 0.18 (CH₂Cl₂/CH₃OH:85/15); ¹H NMR (400 MHz, DMSO-d₆): δ = 1.94-2.06 (m, 2H, CH₂), 2.25-2.33 (m, 1H, CH₂), 2.43-2.47 (m, 1H, CH₂), 2.50-2.57 (m, 2H, CH₂), 5.46 (d, J = 6.8 Hz, 1H, CH*), 7.46 (d, J = 8.4 Hz, 2H, H-Ar_{ortho}), 8.10 (d, 2H, J = 9.2 Hz, H-Ar_{meta}), 8.19 (d, J = 9.2 Hz, 1H, NH-CH*), 11.10 (br s, 1H, NH) ppm; ¹³C NMR (100 MHz, DMSO-d₆): δ = 21.00, 28.05, 36.44, 54.96, 106.79, 122.69, 129.19, 146.46, 147.46, 193.96 ppm; IR (KBr): ν = 3322 (NH), 3114 (NH), 1704 (C=O), 1603 (C=C), 1348 and 1171 (SO₂) cm⁻¹; MS: (m/z) = 297.0 (M+1); Anal. Calc. for C₁₃H₁₃FN₂O₃S: C, 52.69; H, 4.42; N, 9.45; Found: C, 52.63; H, 4.48; N, 9.52.

4-(2-chlorophenyl)-4,6,7,8-tetrahydro-1H-benzo[c][1,2,6]thiadiazin-5(3H)-one 2,2-dioxide
(**5a**, C₁₃H₁₃ClN₂O₃S):

White powder; 91 % yield; R_f = 0.19 (CH₂Cl₂/CH₃OH:85/15); ¹H NMR (400 MHz, DMSO-d₆): δ = 1.91-2.07 (m, 2H, CH₂), 2.27-2.32 (m, 1H, CH₂), 2.34-2.40 (m, 1H, CH₂), 2.53-2.64 (m, 2H, CH₂), 5.58 (d, J = 6.4 Hz, 1H, CH*), 7.02 (td, J₁ = 7.5, J₂ = 1.1 Hz, 2H, H-Ar), 7.11 (ddd, J₁ = 16.4, J₂ = 8.5, J₃ = 1.3 Hz, 1H, H-Ar), 7.27 (ddd, J₁ = 15.3, J₂ = 5.4, J₃ = 1.8 Hz, 1H, H-Ar), 8.02 (d, J = 6.8 Hz, 1H, NH-CH*), 10.97 (br s, 1H, NH) ppm; ¹³C NMR (100 MHz, DMSO-d₆): δ = 20.98, 28.04, 36.53, 49.89, 106.52, 114.68, 114.90, 123.30, 126.38, 126.51, 129.25, 129.88, 158.98, 193.85 ppm; IR (KBr): ν = 3272 (NH), 3126 (NH), 1702 (C=O), 1606

(C=C), 1353 and 1171 (SO₂) cm⁻¹; MS: (m/z) = 313.0 (M+1); Anal. Calc. for C₁₃H₁₃ClN₂O₃S: C, 49.92; H, 4.19; N, 8.96; Found: C, 49.97; H, 4.25; N, 8.89.

4-(4-chlorophenyl)-4,6,7,8-tetrahydro-1H-benzo[c][1,2,6]thiadiazin-5(3H)-one 2,2-dioxide (6a, C₁₃H₁₃ClN₂O₃S):

White powder; 92 % yield; R_f = 0.20 (CH₂Cl₂/CH₃OH:85/15) ; ¹H NMR (400 MHz, DMSO-d₆): δ = 1.92-2.03 (m, 2H, CH₂), 2.22-2.24 (m, 1H, CH₂), 2.25-2.30 (m, 1H, CH₂), 2.37-2.57 (m, 2H, CH₂), 5.31 (d, *J* = 6.8 Hz, 1H, CH*), 7.14 (d, *J* = 8.4 Hz, 2H, H-Ar_{ortho}), 7.42 (d, *J* = 8.4 Hz, 2H, H-Ar_{meta}), 8.02 (d, *J* = 6.8 Hz, 1H, NH-CH*), 10.97 (br s, 1H, NH) ppm; ¹³C NMR (100 MHz, DMSO-d₆): δ = 20.99, 28.04, 36.54, 55.08, 107.32, 119.57, 130.14, 130.39, 139.02, 156.35, 193.72 ppm; IR (KBr): ν = 3431 (NH), 3254 (NH), 1701 (C=O), 1601 (C=C), 1352 and 1169 (SO₂) cm⁻¹; MS: (m/z) = 313.0 (M+1); Anal. Calc. for C₁₃H₁₃ClN₂O₃S: C, 49.92; H, 4.19; N, 8.96; Found: C, 49.84; H, 4.23; N, 8.88.

4-(2-bromophenyl)-4,6,7,8-tetrahydro-1H-benzo[c][1,2,6]thiadiazin-5(3H)-one 2,2-dioxide (7a, C₁₃H₁₃BrN₂O₃S):

Yellow powder; 89 % yield; R_f = 0.20 (CH₂Cl₂/CH₃OH:85/15) ; ¹H NMR (400 MHz, DMSO-d₆): δ = 1.92-2.15 (m, 2H, CH₂), 2.21-2.23 (m, 1H, CH₂), 2.24-2.28 (m, 1H, CH₂), 2.33-2.60 (m, 2H, CH₂), 5.60 (d, *J* = 7.2 Hz, 1H, CH*), 7.03 (td, *J*₁ = 8.5, *J*₂ = 1.1 Hz, 1H, H-Ar), 7.13 (tdd, *J*₁ = 9.4, *J*₂ = 7.9, *J*₃ = 1.3 Hz, 2H, H-Ar), 7.28 (ddd, *J*₁ = 15.3, *J*₂ = 5.4, *J*₃ = 1.8 Hz, 1H, H-Ar), 8.02 (d, *J* = 7.0 Hz, 1H, NH-CH*), 10.98 (br s, 1H, NH) ppm; ¹³C NMR (100 MHz, DMSO-d₆): δ = 21.19, 28.28, 36.71, 50.11, 106.76, 114.90, 123.51, 126.62, 129.38, 130.06, 159.20, 193.72 ppm; IR (KBr): ν = 3254 (NH), 3119 (NH), 1702 (C=O), 1605 (C=C), 1355 and 1171 (SO₂) cm⁻¹; MS: (m/z) = 357.0 (M+1), 359.0 (M+1+2); Anal. Calc. for C₁₃H₁₃BrN₂O₃S: C, 43.71; H, 3.67; N, 7.84; Found: C, 43.76; H, 3.71; N, 7.88.

4-(4-bromophenyl)-4,6,7,8-tetrahydro-1H-benzo[c][1,2,6]thiadiazin-5(3H)-one 2,2-dioxide (8a, C₁₃H₁₃BrN₂O₃S):

Yellow powder; 90 % yield; R_f = 0.20 (CH₂Cl₂/CH₃OH:85/15) ; ¹H NMR (400 MHz, DMSO-d₆): δ = 1.92-2.15 (m, 2H, CH₂), 2.27-2.30 (m, 1H, CH₂), 2.37-2.43 (m, 1H, CH₂), 2.50-2.57 (m, 2H, CH₂), 5.32 (d, *J* = 6.4 Hz, 1H, CH*), 7.14 (d, *J* = 8.4 Hz, 2H, H-Ar), 7.42 (d, *J* = 7.2 Hz, 2H, H-Ar), 8.02 (d, *J* = 6.8 Hz, 1H, NH-CH*), 10.97 (br s, 1H, NH) ppm; ¹³C NMR (100 MHz, DMSO-d₆): δ = 21.16, 27.06, 36.28, 55.08, 107.32, 119.97, 130.14, 130.39, 139.03, 156.60, 193.73 ppm; IR (KBr): ν = 3253 (NH), 3128 (NH), 1703 (C=O), 1602 (C=C), 1354

and 1170 (SO₂) cm⁻¹; MS: (m/z) = 357.0 (M+1), 359.0 (M+1+2); Anal. Calc. for C₁₃H₁₃BrN₂O₃S: C, 43.71; H, 3.67; N, 7.84; Found: C, 43.67; H, 3.70; N, 7.86.

4-(2-hydroxyphenyl)-4,6,7,8-tetrahydro-1H-benzo[c][1,2,6]thiadiazin-5(3H)-one 2,2-dioxide
(9a, C₁₃H₁₄N₂O₄S):

White powder; 91 % yield; R_f = 0.20 (CH₂Cl₂/CH₃OH:85/15); ¹H NMR (400 MHz, DMSO-d₆): δ = 1.91-2.04 (m, 2H, CH₂), 2.20-2.27 (m, 1H, CH₂), 2.32-2.39 (m, 1H, CH₂), 2.50-2.62 (m, 2H, CH₂), 5.62 (d, *J* = 7.2 Hz, 1H, CH*), 7.15-7.25 (m, 2H, H-Ar), 7.24-7.26 (m, 1H, H-Ar), 7.40 (d, *J* = 8.00 Hz, 1H, H-Ar), 8.08 (d, *J* = 7.2 Hz, 1H, NH-CH*), 10.96 (br s, 1H, NH) ppm; ¹³C NMR (100 MHz, DMSO-d₆): δ = 21.00, 28.02, 36.57, 53.23, 107.03, 126.16, 128.96, 129.04, 130.06, 131.05, 133.05, 136.37, 156.78, 193.66 ppm; IR (KBr): ν = 3235 (OH), 3124 (NH), 1701 (C=O), 1639 (C=C), 1354 and 1170 (SO₂) cm⁻¹; MS: (m/z) = 312.2 (M+H₂O); Anal. Calc. for C₁₃H₁₄N₂O₄S: C, 53.05; H, 4.79; N, 9.52; Found: C, 53.11; H, 4.84; N, 9.50.

4-(4-nitrophenyl)-4,6,7,8-tetrahydro-1H-benzo[c][1,2,6]thiadiazin-5(3H)-one 2,2-dioxide
(10a, C₁₃H₁₃N₃O₅S):

White powder; 82 % yield; R_f = 0.19 (CH₂Cl₂/CH₃OH:85/15); ¹H NMR (400 MHz, DMSO-d₆): δ = 1.92-2.03 (m, 2H, CH₂), 2.22-2.28 (m, 1H, CH₂), 2.33-2.39 (m, 1H, CH₂), 2.48-2.57 (m, 2H, CH₂), 5.59 (d, *J* = 7.2 Hz, 1H, CH*), 7.02 (td, *J*₁ = 7.5, *J*₂ = 1.1 Hz, 1H, H-Ar_{ortho}), 7.06-7.16 (m, 2H, H-Ar_{meta+para}), 7.27 (tdd, *J*₁ = 7.2, *J*₂ = 5.4, *J*₃ = 1.8 Hz, 1H, *), 8.04 (d, *J* = 7.0 Hz, 1H, NH-CH*), 10.97 (br s, 1H, NH) ppm; ¹³C NMR (100 MHz, DMSO-d₆): δ = 20.98, 28.04, 36.52, 49.91, 106.60, 114.70, 114.91, 123.31, 126.40, 129.27, 129.88, 159.00, 193.61 ppm; IR (KBr): ν = 3220 (NH), 3134 (NH), 1705 (C=O), 1606 (C=C), 1356 and 1172 (SO₂) cm⁻¹; MS: (m/z) = 324.0 (M+1); Anal. Calc. for C₁₃H₁₃N₃O₅S: C, 48.29; H, 4.05; N, 13.00; Found: C, 48.34; H, 4.11; N, 13.08.

4-(naphthalen-1-yl)-4,6,7,8-tetrahydro-1H-benzo[c][1,2,6]thiadiazin-5(3H)-one 2,2-dioxide
(11a, C₁₇H₁₆N₂O₃S)

Red powder; 84 % yield; R_f = 0.28 (CH₂Cl₂/CH₃OH:85/15); ¹H NMR (400 MHz, DMSO-d₆): δ = 1.96-2.08 (m, 1H, CH₂), 2.09-2.27 (m, 1H, CH₂), 2.28-2.34 (m, 1H, CH₂), 2.44-2.50 (m, 1H, CH₂), 2.55-2.64 (m, 2H, CH₂), 5.52 (d, *J* = 6.4 Hz, 1H, CH*), 7.43-7.47 (m, 3H, H-Ar), 7.57 (s, 1H, H-Ar), 7.79 (d, *J* = 8.5 Hz, 1H, H-Ar), 7.84-7.86 (m, 2H, H-Ar), 8.07 (d, *J* = 6.6 Hz, 1H, NH-CH*), 10.92 (br s, 1H, NH) ppm; ¹³C NMR (100 MHz, DMSO-d₆): δ = 21.03, 28.16, 36.63, 55.68, 107.75, 125.68, 125.77, 126.17, 126.57, 126.97, 127.36, 127.86, 132.28, 132.52, 137.03, 156.35, 193.07 ppm; IR (KBr): ν = 3410 (NH), 3262 (NH), 1708 (C=O), 1601

(C=C), 1358 and 1172 (SO₂) cm⁻¹; MS: (m/z) = 329.1 (M+1); Anal. Calc. for C₁₇H₁₆N₂O₃S: C, 62.18; H, 4.91; N, 8.53; Found: C, 62.26; H, 4.96; N, 8.55.

4-(4-(trifluoromethyl)phenyl)-4,6,7,8-tetrahydro-1H-benzo[c][1,2,6] thiadiazin-5(3H)-one 2,2-dioxide (**12a**, C₁₄H₁₃F₃N₂O₃S):

White powder; 88 % yield; R_f = 0.21 (CH₂Cl₂/CH₃OH:85/15); ¹H NMR (400 MHz, DMSO-d₆): δ = 1.68-1.82 (m, 2H, CH₂), 1.83-1.86 (m, 1H, CH₂), 1.89-2.02 (m, 1H, CH₂), 2.15-2.48 (m, 2H, CH₂), 5.07 (s, 1H, CH*), 6.75-7.08 (m, 3H, H-Ar), 7.10-7.13 (m, 1H, H-Ar), 7.14-7.21 (m, 1H, NH-CH*), 10.47 (br s, 1H, NH) ppm; ¹³C NMR (100 MHz, DMSO-d₆): δ = 20.40, 27.26, 36.67, 48.11, 101.16, 111.58, 115.52, 121.38, 124.24, 129.27, 150.12, 166.99, 196.00 ppm; IR (KBr): ν = 3225 (NH), 3116 (NH), 1702 (C=O), 1598 (C=C), 1354 and 1170 (SO₂) cm⁻¹; MS: (m/z) = 324.0 (M+1); Anal. Calc. for C₁₃H₁₃N₃O₅S: C, 48.55; H, 3.78; N, 8.09; Found: C, 48.62; H, 3.84; N, 8.13.

2.2. Biological assays

2.2.1. Anticholinesterase assay

2.2.1.1. Chemicals

All used chemicals were of analytical reagent grade. Acetylcholinesterase (AChE, lyophilized powder), acetylthiocholine iodide (ATCI), butyrylcholinesterase (BuChE, lyophilized powder), butyrylthiocholine iodide (BTCI), and 5,5'-dithio-bis-(2-nitrobenzoic acid) (DTNB) were purchased from Sigma- Aldrich (MO, USA).

2.2.1.2. AChE and BuChE inhibitory assay

The inhibitory activity of AChE and BuChE was determined using an *in vitro* microplate assay developed by *Ellman et al* [21]. Each molecule was dissolved in MeOH (4mM) and diluted to various concentrations before use. Briefly, 150 μL of sodium phosphate buffer (0.1M, pH 8.0) were mixed with 10 μL of each sample and 20 μL of AChE (5.32x10⁻³ U) or BuChE (6.85x10⁻³ U). The mixture was incubated at 25°C for 15 min. Then, 10 μL of DTNB (0.5 mM) and 10 μL of acetylthiocholine iodide (ACI, 0.71 mM) or butyrylthiocholine chloride (BCI, 0.2mM) were added. The absorbance was measured in 412 nm against a negative control using a microplate reader (PerkinElmer, EnSpire Multimode Plate Reader, USA) and the inhibition rate was determined for each concentration. Galantamine was used as a reference drug and all tests were evaluated in triplicate.

2.2.1.3. Statistical analysis

The results were expressed as mean±SD of three parallel measurements. The analysis and drawing were realized using GraphPad prism (software, San Diego, CA, USA). Comparison between IC₅₀ values were analyzed by ANOVA one way followed by Tuckey post-hoc test. The difference was considered statistically significant when the *P* value was less than 0.05

2.3. *In silico* study

2.3.1. Molecular Docking

The X-ray crystal structure of AChE in complex with galantamine (Protein Data Bank ID: 4EY6) [22] were obtained from the RSC Protein Data Bank, and were prepared with protein preparation wizard in Schrodinger suites. The three-dimensional structures of the derivatives were constructed using Maestro software, and prepared with Ligprep using OPLS3e force field. [23]

The final prepared PDB file of the protein and synthesized compounds were submitted in order to run docking process. Docking studies were performed by Glide software [24] at extra precision [25]. Output files of docked compounds were visualized on Chimera software [26].

2.3.2. Molecular Dynamics

Molecular Dynamics simulations (MD) were performed using Desmond [27]. The best docking complex for the identified inhibitors from the biological experiments were taken as the initial coordinates for MD simulations. A 10 Å cubic water box employing the TIP3P water model was used for the solvation of the system with OPLS3e force field. Sodium ions were added as counter ions to neutralize the systems. We have then subjected the system to minimization using an energy gradient convergence threshold of 1 kcal/mol/Å and pre-equilibration using the default six-step relaxation protocol implemented in Desmond. The first two steps are minimization steps, one in which solute is kept restrained while another without restraints. Further, steps three to six are short MD simulations of 12 ps, 12 ps, and 24 ps each using the NPT ensemble at 10, 10, 300, and 300 K, respectively. Subsequently, a 100 nanosecond (ns) MD simulation production run was performed. Remaining parameters were kept at the Desmond default values. We have visualized the protein-ligand complexes and analyzed the MD trajectory using Maestro. The detailed analyses were performed using the Simulation Event Analysis tool of Desmond.

3. Results and discussion

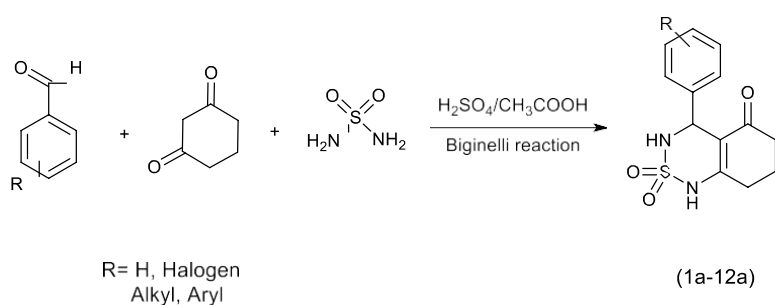
3.1. Chemistry

In order to further our research on the development and synthesis of bioactive compounds [28] using modern and efficient synthesis techniques such as ultrasound and microwave irradiation [29], we have expanded our investigations by synthesizing heterocyclic compounds containing the sulfamide moiety.

The synthesis of these heterocyclic compounds (also called cyclosulfamides) was carried out in a single step *via* the Biginelli cyclo-condensation reaction.

Synthesized derivatives of cyclosulfamide are obtained from a reaction between various aromatic aldehydes, cyclohexanedione, and sulfamide in the presence of a catalytic amount of $\text{H}_2\text{SO}_4/\text{CH}_3\text{COOH}$ (1/9) under microwave irradiation and solvent-free condition at room temperature [30].

The target compounds (**1a-12a**) reacted very well, giving excellent yields (82-92%) in short reaction times (5-10min) (Scheme 1).



Scheme 1. Synthesis of cyclosulfamide derivatives *via* Biginelli reaction under microwave irradiation.

The structures of the synthesized cyclosulfamides (**1a-12a**) are presented in Table 1.

Table 1. Structures of synthesized derivatives of cyclosulfamide.

Code	1a	2a	3a	4a	5a	6a
Structure						
Code	7a	8a	9a	10a	11a	12a
Structure						

3.2. Biological results

3.2.1. *In vitro* Anticholinesterase activity

In parallel to cognitive and behavioral disorders, several biochemical events were observed in AD patients, decreasing in ACh levels, aggregation of β -amyloid peptide (β A), increasing in intracellular phosphorylation, dys-regulation of metallic ions and mitochondrial dysfunctions. [5,31]. AChE (EC.3.1.1.7) is an important enzyme in the modulation of cholinergic transmission through synaptic Acetylcholine hydrolysis. BuChE (EC.3.1.1.8) participated in the stability of nerve signal by compensation of AChE activity [32]. Actually, no specific treatment for this multifactorial disease, but the cholinergic hypothesis remained the most powerful theory in the development of novel anti-Alzheimer's drugs, through inhibition of both AChE and BuChE [33]. Moreover, the presence of sulfamide unit in heterocyclic structures offered potent alternatives with high therapeutic efficiency in medical practice. Many reports revealed the antibacterial, antidiabetic, and antitrypanosomal activities of sulfamides [2]. This study is focused on cyclosulfamide derivatives, in the first hand, due to their ability to affect the central neurons system and generating several effects such as anticonvulsion, treatment of depression and reduction of inflammatory and neurologic pain, consequently, the ability to improve some neuronal dysfunctions in AD patients [34,4]. In another hand, the enzymatic inhibitory activity of cyclosulfamides is widely reported especially against HIV-1 proteases, tyrosine kinase, human elastase and particularly serine proteases such as AChE and BuChE [35,36]. In this context, the anticholinesterase activity of novel synthetic cyclosulfamides were evaluated.

The inhibitory activity of studied cyclosulfamide-based derivatives was determined as IC_{50} values (μ M) and mentioned in Table 2. The structural diversity of these compounds radically influenced the activity against AChE and BuChE. For AChE inhibition, the IC_{50} ranged from 45.30 ± 0.88 to >200 μ M. The basic compound **1a** showed a moderate activity ($IC_{50} = 125.08 \pm 2.69$ μ M). The addition, in different positions, of halogen atoms such as fluorine in **2a**, **3a**, **4a** and chloride in **5a** and **6a** reduced the activity and made them inactive. Moreover, the addition of bromine atoms in **7a** slightly improved the activity ($IC_{50} = 119.92 \pm 1.61$ μ M) while, in **8a** the activity was reduced. An interesting activity was recorded for compounds **10a** ($IC_{50} = 45.30 \pm 0.88$ μ M) and **12a** ($IC_{50} = 116.34 \pm 1.37$ μ M) which showed the greatest activity of the series. Other compounds **9a** and **11a** were considered inactive. Galantamine exhibited the best inhibitory effect.

In BuChE inhibitory activity, the behavior of molecules changed and the efficiency clearly appeared. The IC₅₀ values ranged from 52.87±3.73 to >200 μM and the basic molecule **1a** showed a moderate activity (IC₅₀=137.87±0.64μM). Compounds **2a**, **4a**, **6a**, **9a**, **11a** which were inactive in AChE assay exhibited a potent BuChE inhibition. The most potent one was the fluorine substituted **4a** (IC₅₀=52.87±3.73 μM). In another hand, **7a** and **12a** molecules showed an opposite effect, the great efficiency against AChE has become inactive to BuChE. Compounds **3a** and **8a** remained inactive against dual AChE and BuChE. In addition, the selectivity indexes of studied compounds against both enzymes showed a **more** important selectivity for BuChE (**2a**, **4a**, **5a**, **6a**, **7a**, **9a**, **11a**) than AChE (**1a**, **10a**, **12a**). Compounds **3a** and **8a** revealed inactive non-selective (Table 2).

Table 2. Anticholinesterase activity and enzymatic selectivity of tested compounds.

Compound Code	Anticholinesterase activity		Selectivity index	
	AChE	BuChE	AChE	BuChE
1a	125.08±2.69	137.87±0.64	0.90	1.10
2a	>200	102.96±1.76	1.21	0.82
3a	>200	>200	2.36	0.42
4a	>200	052.87±3.73	>1.94	<0.51
5a	153.58±0.93	064.90±0.06	>1.19	<0.83
6a	>200	147.67±0.88	>1.00	>1.00
7a	119.92±1.61	098.66±1.38	3.17	0.31
8a	>200	>200	>3.78	<0.26
9a	>200	166.57±2.32	<0.58	>1.71
10a	045.30±0.88	>200	<0.22	>4.41
11a	199.01±1.01	147.67±0.88	>1.35	<0.73
12a	116.34±1.37	>200	>1.00	>1.00
Galantamine	002.10±0.07	020.38±2.10	0.10	9.70

IC₅₀ values represent the means ± SD. of three parallel measurements (p<0.05).

Galantamine: Reference drug.

The blockage of AChE improved the level of ACh in different brain parts and attenuated temporarily the cognitive disorders [34]. Molecules that inhibited the anionic catalytic site (ACS) and the peripheral anionic site (PAS) revealed as potent therapeutic drugs [37]. Several studies reported the involvement of BuChE inhibitors in the treatment of AD especially in the

late stage. Then, it modulates the AChE levels in different states. Therefore, the best management of AD symptoms requires the dual inhibition of both enzymes [38].

Many reports discussed the correlation between the inhibitory effects against cholinesterase enzymes with aromatic ring of inhibitors and the presence of aliphatic chains in active compounds [6]. Thus, the integration of halogen atoms in the aromatic ring, in different positions, improved the therapeutic effect by utilizing of tensile and steric effects of the halogen bonds to occupy the binding sites of molecular targets, as well as, the potent sensitivity of C-X (Cl, Br, F, I) to steric factors [39]. Additionally, due to their lipophilicity and permeability properties, the addition of halogens improved the pharmacokinetic and pharmacodynamics properties of drugs, especially those affecting the central nerves system (CNS) for AD treatment [39].

3.3. *In silico* Study

3.3.1. Molecular docking

To investigate and explain the binding mode and interactions between the targeted protein and synthesized ligands, a molecular docking study was carried out.

We used the Schrodinger suite (version 11.8) and UCSF Chimera (version 1.13.1) programs for our study, and Galantamine was taken as a reference ligand.

The precision of the docking protocol was evaluated by re-docking of Galantamine in the active site of AChE enzyme.

Figure 2 illustrates docked Galantamine and co-crystallized one in nearly identical positions among the receptor (RMSD = 0.42), confirming the validation of docking protocol using Extra Precision scoring function in the absence of water molecules.

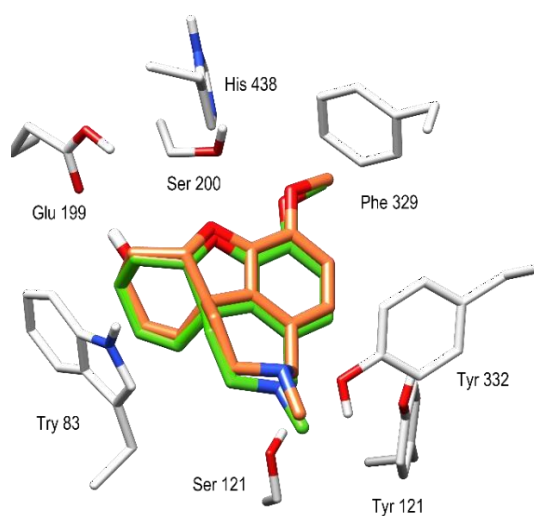


Figure 3. Docked and co-crystallized Galantamine in AChE enzyme after self-docking calculation.

The results of this study including the estimated glide score of the docked positions are provided in **Figure 4** and **Table 3**.

According to molecular docking studies, all synthesized ligands **showed** significant stability in the active site due to the formation of important hydrogen bonds, hydrophobic interactions, and electrostatic attraction forces.

Compounds **10a**, **11a** and **5a** gave a better glide score when compared with Galantamine for the target protein, with binding score of -7.82kcal/mol, -7.86kcal/mol, and -7.89 kcal/mol respectively, and the other compounds **showed** a docking score in the range of -6.89kcal/mol and -7.60kcal/mol **which is** less than the reference ligand docking score.

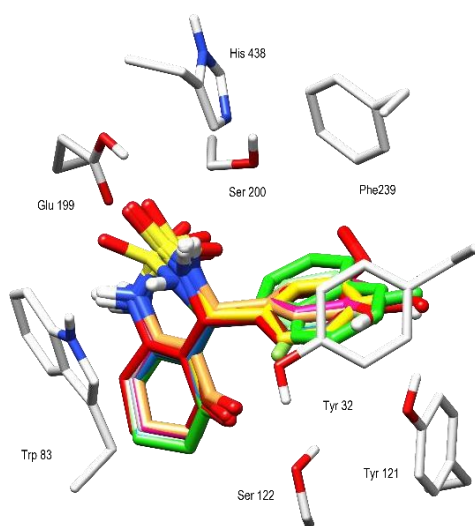


Figure 4. Super imposition of docked derivatives in the active site of AChE enzyme.

Table 3. Docking score (kcal/mol) of synthesized cyclosulfamides (**1a-12a**) with the reference compound 'Galantamine' against AChE enzyme.

Compound code	Docking score
1a	-7.22
2a	-7.12
3a	-7.02
4a	-7.54
5a	-7.89
6a	-7.60
7a	-6.90

8a	-7.11
9a	-7.13
10a	-7.82
11a	-7.86
12a	-6.89
Galantamine	-7.72

The binding interaction of synthesized cyclosulfamides (**1a-12a**) and Galantamine against AChE enzyme were reported in [Table 4](#).

Table 4. Analysis of binding interaction of synthesized cyclosulfamides (**1a-12a**) and the reference ligand against AChE enzyme.

Comp code	Hydrogen bond	Hydrophobic interaction
1a	Glu202, Ser203	Phe295, Phe297, Tyr124, Tyr337, Phe338, Tyr341, Trp86, Tyr133, Ile451, Leu130, Ala127, His447
2a	Glu202	Phe295, Phe297, Tyr124, Tyr337, Phe338, Tyr341, Trp86, Tyr133, Ala204, Ile451, His447
3a	Glu202, Tyr133	Phe295, Phe297, Tyr124, Tyr337, Phe338, Tyr341, Trp86, Tyr133, Ala204, Ile451, His447
4a	Glu202, Ser203	Phe295, Phe297, Tyr124, Tyr337, Phe338, Tyr341, Trp86, Tyr133, Ala204, Ile451, His447
5a	Tyr337, Tyr124	Phe295, Phe297, Tyr124, Tyr337, Phe338, Tyr341, Trp86, Tyr133, Ala204, Ile451, His447
6a	Tyr337, Glu202, Ser203	Phe295, Phe297, Tyr124, Tyr337, Phe338, Tyr341, Trp86, Tyr133, Ala204, Ile451, His447
7a	Tyr124	Phe295, Phe297, Tyr124, Tyr337, Phe338, Tyr341, Trp86, Tyr133, Ala204, Ile451, His447
8a	Tyr337, Ser203	Phe295, Phe297, Tyr124, Tyr337, Phe338, Tyr341, Trp86, Tyr133, Ala204, Ile451, His447
9a	Tyr337, Tyr124	Phe295, Phe297, Tyr124, Tyr337, Phe338, Tyr341, Trp86, Tyr133, Ala204, Ile451, His447

10a	Tyr337, Tyr124, Ser203, Tyr341	Phe295, Phe297, Tyr124, Tyr337, Phe338, Tyr341, Trp86, Tyr133, Ala204, Ile451, His447
11a	Glu202	Phe295, Phe297, Tyr124, Tyr337, Phe338, Tyr341, Trp86, Tyr133, Ala204, Ile451, His447
12a	Ser203	Phe295, Phe297, Tyr124, Tyr337, Phe338, Tyr341, Trp86, Tyr133, Ala204, Ile451, His447
Galantamine	Tyr337, Glu202, Ser203	Phe295, Phe297, Tyr124, Tyr337, Phe338, Tyr341, Trp86, Tyr133, Ala204, Ile451, His447

Following the visualization of molecular docking results using the Chimera program, most of synthesized compounds form hydrogen bonds with **Tyr337**, **Glu202**, and **Ser203** as the binding of the reference ligand residues. Further, these compounds form additional critical hydrogen bond with **Tyr124** residue.

The benzaldehyde-derived compound **1a** shows significant stability in the active pocket of AChE enzyme due to the formation of two hydrogen bonds with Glu202 and Ser203 as well as hydrophobic interactions with Phe295, Phe297, Trp86, and His447 residues that are responsible for the inhibition of AChE enzyme.

The best **in vitro inhibitor** of AChE enzyme **10a** ($IC_{50}=0.45.30\pm 0.88\mu M$) showed a better stability *in silico* (-7.82kcal/mol) than the reference ligand (-7.72kcal/mol) in the active site because of the formation of four hydrogen bonds with Tyr337, Tyr124, Tyr 341 and Ser203. Also, **10a** interacts with Phe295, Phe297, Trp86, and His447 residues in a hydrophobic manner.

The binding mode of the compound **5a** positioned in the AChE active site showed that Tyr337 and Tyr124 residues form two hydrogen bonds with nitrogen atoms of the cyclosulfamide ring, and His447 residue forms a halogen bond with the chlorine of the aromatic group. Moreover, the phenyl and cyclosulfamide groups of **5a** form π - π stacking with Trp86, while the residues such as Phe295, Phe297, Phe338, Tyr341, Tyr133, and Ala204 form hydrophobic interactions with the cyclohexenone and phenyl rings of compound **5a**.

Compound **11a** also shows significant stability in the active site of AChE and moderate *in vitro* inhibition ($IC_{50}=199\mu M$) despite forming only one hydrogen bond with Glu202.

We observed that the two aromatic rings of **11a** increase its stability in the active pocket and that due to the formation of two π - π staking with Tyr337 and Phe338 residues, and many crucial

hydrophobic interactions such as Phe295, Phe297, Tyr124, Tyr337, Phe338, Tyr341, Trp86, His447.

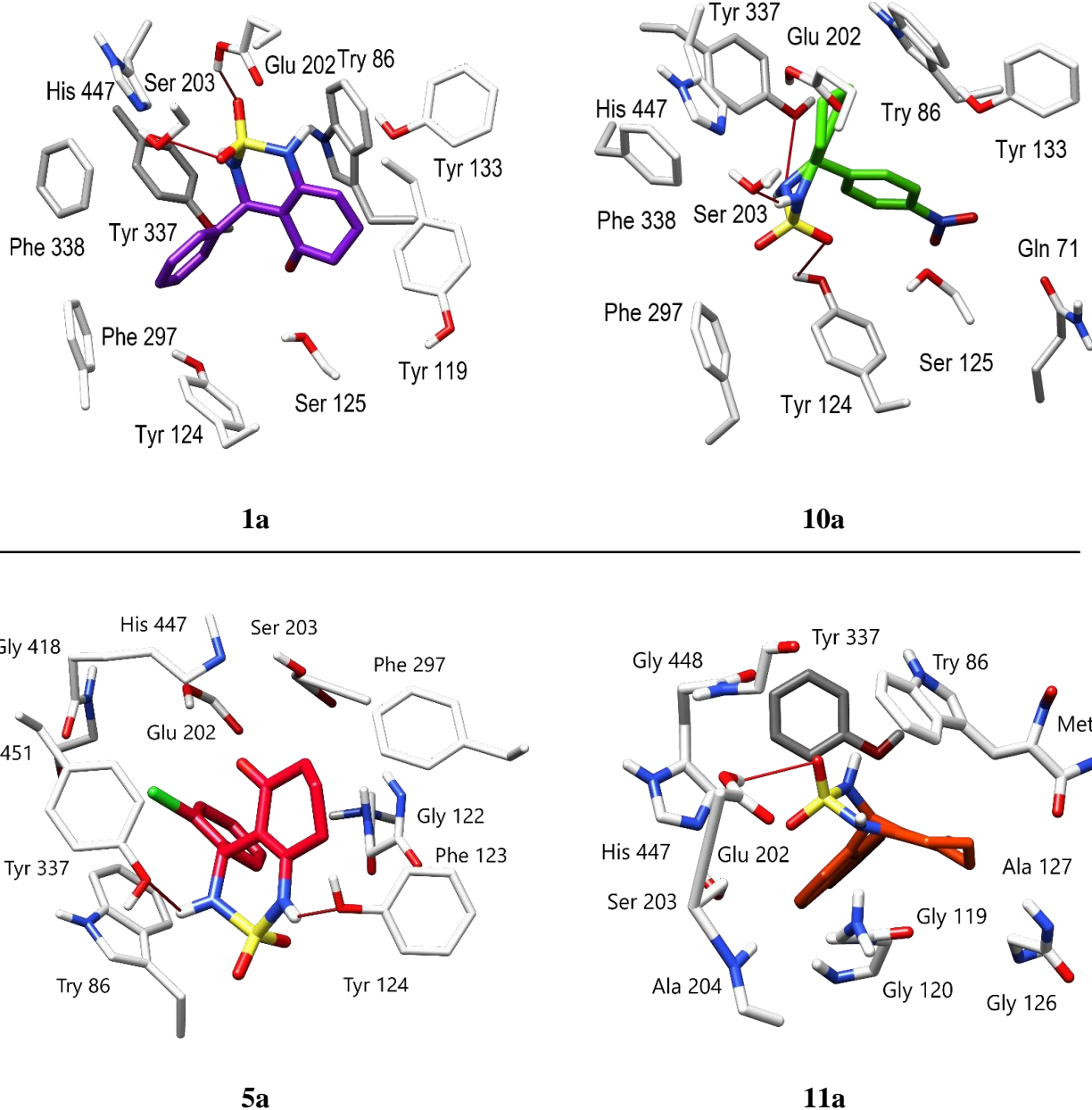


Figure 5. 3D binding disposition of **1a**, **5a**, **10a**, and **11a** after docking calculations in the active site of AChE enzyme. The amino acid residues were shown as white stick model and H-bonds were shown as red lines.

Molecular docking analysis showed that most of studied compounds interact with the active site of AChE in a very efficient and satisfactory manner, emphasizing the importance of the

presence of the cyclosulfamide moiety as well as aromatic ring substituted by nitrogen dioxide or substituted by another aromatic group.

3.3.2. Molecular dynamic (MD) simulation

The complex structure containing the **10a** ligand bound with AChE was taken to perform the molecular dynamic (MD) simulation. The molecular dynamic simulation was conducted using the free Desmond academic software-2022 and OPLS-2005 force field implemented on the LINUX environment's Intel Xeon Octal-Core 2.88 Mhz. The AChE-**10a** ligand complex was solvated in an orthorhombic box with a dimension of 10.0x10.0x10.0 nm³. The simulation box contains 51182 Atoms, 14330 TIP3P water molecules, and 530 residues. The net charge of the complex system was neutralized by 8 molecules of Na⁺. All protein atoms were maintained at a distance equal to 10 Angstroms from the solvate box edges. The solvated system was subjected to energy minimization of 50000 steps. After performing the energy minimization, the minimized system was equilibrated for 100ps at 300K. Following equilibration, the system was subjected to a final production run of 100ns MD simulations at 300K temperatures. Periodic boundary conditions were applied under isothermal and isobaric conditions with a relaxation time of 0.2ps.

3.3.2.1. Root mean square deviation (RMSD) analysis

Structural changes, specifically the deviation between two compositions such as protein and ligand, can be best interpreted by measuring the protein-ligand Root Mean Square Deviation (PL-RMSD) obtained from the MD simulation trajectories. [40] The PL-RMSD measures the scale of distance between the protein and its ligand throughout the simulation time. In this study, all protein frames (1000 frames) are first aligned on the reference frame backbone (frame 0), and then the RMSD is calculated based on the C-Alpha. The RMSD of the protein provide insights into the structural conformations throughout the simulation. It can indicate if the simulation is equilateral, and its fluctuations throughout the simulation are around some thermal average. Changes in the order of one to three angstroms are perfectly acceptable for small molecules [41]. Thus, a high RMSD value indicates the instability of the protein system. In this research work, the comparative RMSD pattern analysis between the **10a** ligand bound to the AChE protein demonstrate that both compositions showed a regular scale of distance throughout the simulation time (Figure 6). From the first frame (0.10ns) to the last frame (100ns) of the molecular dynamic (MD) simulation trajectory, a relative deviation of around

1.25 Angstroms was observed between both RMSD values which is an indicator of the stability of the receptor-ligand complex.

The result indicates that the AChE protein has a periodic backbone stability throughout the MD simulation while bound with the **10a** ligand.

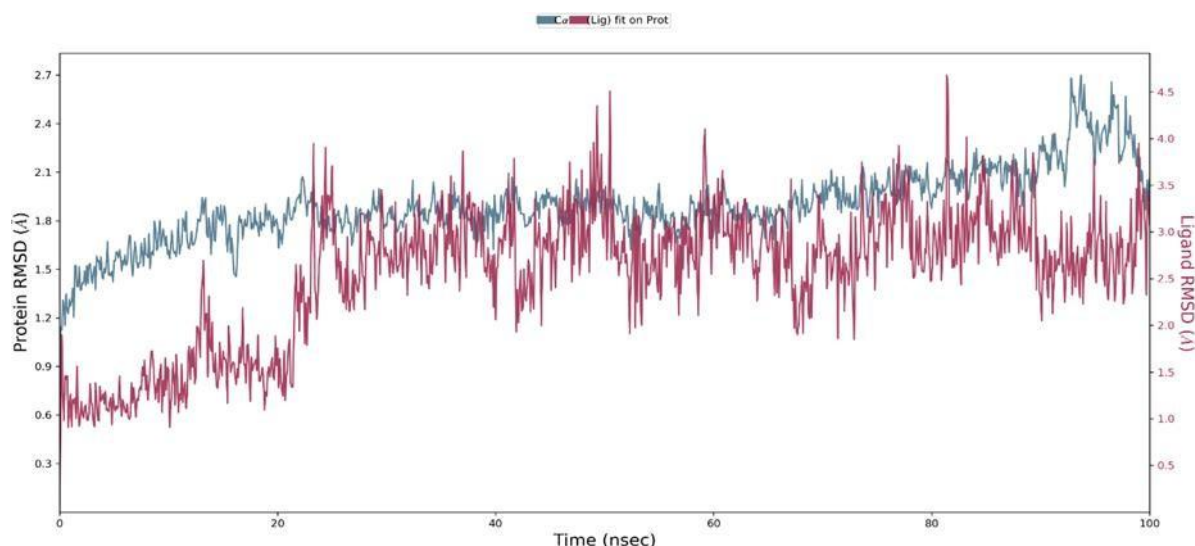


Figure 6. Protein and ligand root mean square deviation (PL-RMSD) obtained from the molecular dynamic simulation trajectories.

3.3.2.2. Root mean square fluctuation (RMSF)

The RMSF is an essential result for measuring the deviation from a reference position of a ligand atom during the simulation time. This parameter represents the average deviation for each residue compared to the same atoms of the reference structure. Indeed, **Figure 7** shows the RMSF diagram of the amino acids of the AChE protein in the studied system. The results were compared with the atomic displacement factor "B factor" of the C_{α} atoms of each residue of the studied protein. On this plot, peaks indicate areas of the protein that fluctuate the most during the simulation. In addition, we observe that the tails (N- and C-terminal) fluctuate more than any other part of the protein. Indeed, the residues: Pro25 (1.77 Å), Ser57 (1.32 Å), Gln66 (1.45 Å), Pro78 (4.16Å), Asn265 (2.19Å), Trp385 (2.35Å), Leu386 (3.09Å), Asp494 (4.70Å), Lys538 (2.08Å) and Ser541 (2.75Å), have higher RMSF values of alpha carbons (C_{α}). Therefore, the comparison of the RMSF curve of the alpha carbons (C_{α}) of the protein with the curve of the atomic displacement factor "B-factor" indicates a good simulation since the curve is parallel to that "B-factor" throughout the 100ns molecular dynamic simulation (**Figure 7**).

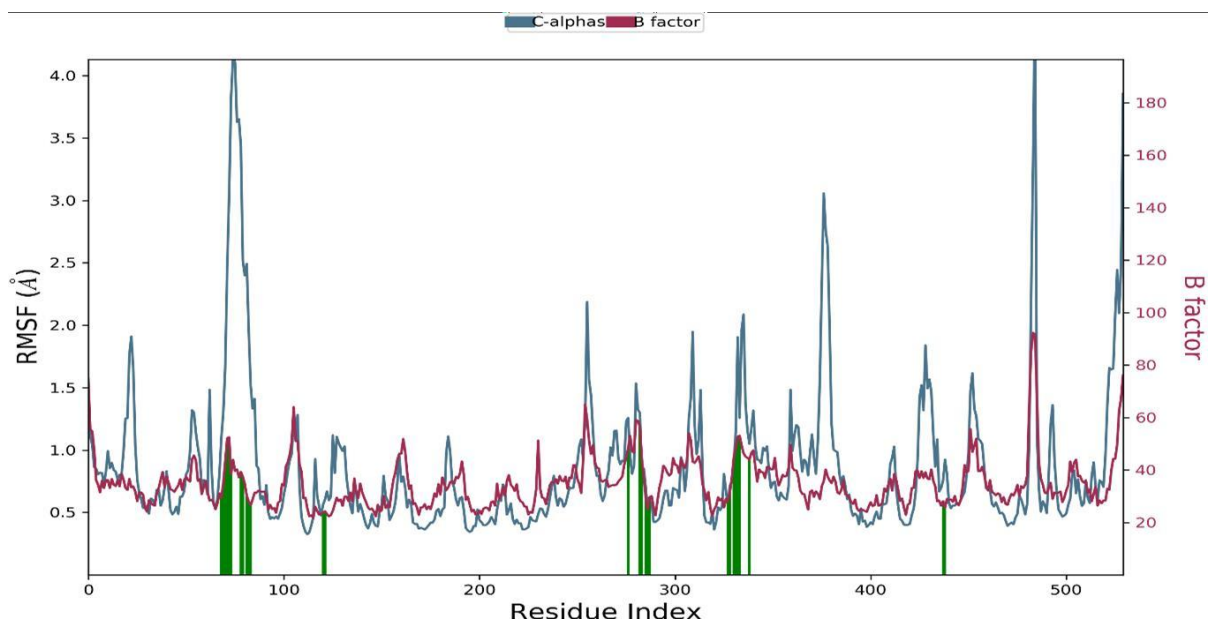


Figure 7. RMSF diagram of the amino acids of the AChE protein in the studied system.

(Protein residues that interact with the ligand are marked with green-colored vertical bars)

3.3.2.3. Hydrogen bond analysis

Hydrogen Bonds (H-bonds) play a significant role in ligand binding. Therefore, consideration of hydrogen-bonding properties in drug design is essential because of their strong influence on drug specificity, metabolism, and adsorption. [42] In our research, the number of Hydrogen bonds formed between the **10a** ligand and AChE-enzyme during the 100ns of molecular dynamic simulation is summed up in **Figure 8**. Results analysis shows that the ligand formed 3 to 5 hydrogen bonds on average, with the residues of the active site of the AChE during the 100ns of molecular dynamic simulation (**Tyr124** 52%, **Phe295** 46%, **Tyr337** 55%, **Tyr341** 5.5%, and **Asn87** 0.6%). The adopted position of the **10a** ligand in the active site of the AChE deployed more interactions, including the following low-energy interactions: Hydrophobic interaction (Trp86, Trp286, Phe297, Phe338, Tyr341) and a multitude of Water bridges interactions. In addition to hydrogen bonds, these low-energy interactions stabilize ligand binding in the protein's active site. This result confirms the potent inhibition of the AChE by the synthesized inhibitor **10a**, thus supporting the results already obtained by the docking, having predicted four hydrogen bonds with the residues of the active site of the AChE.

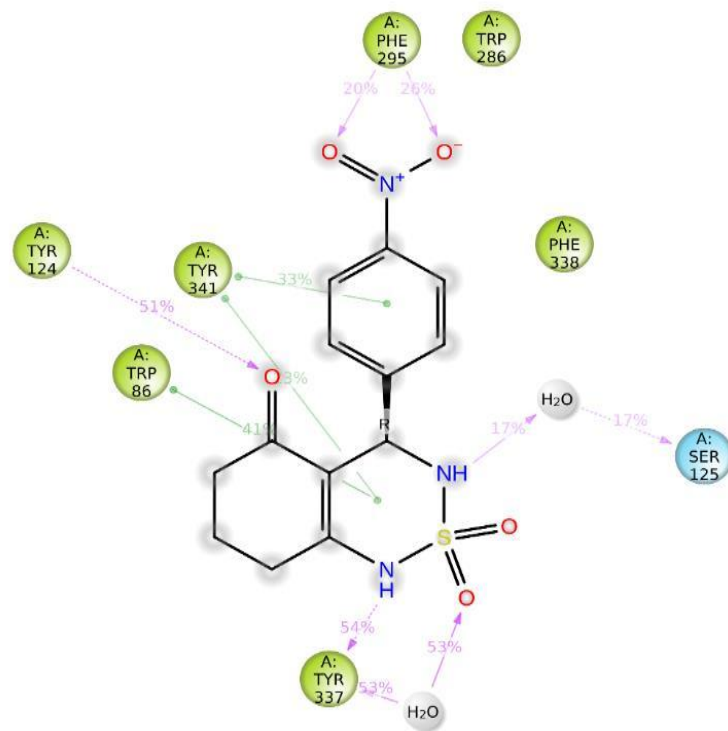
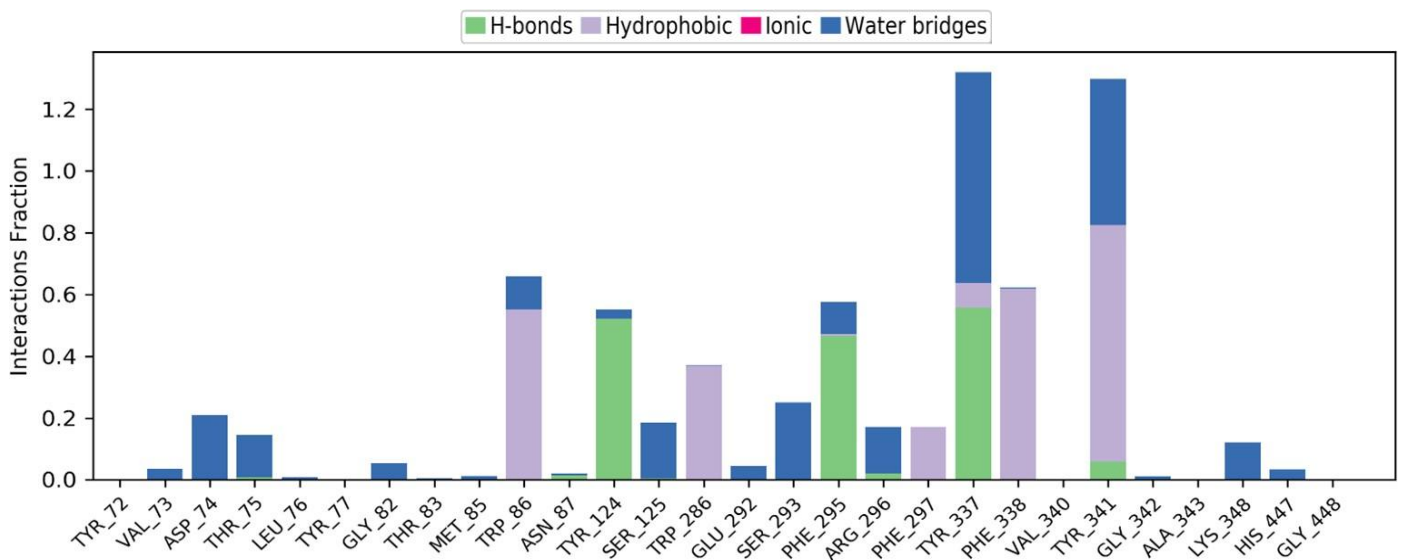


Figure 8. Protein and Ligand Hydrogen bonds contacts obtained from the molecular dynamic simulation trajectories.

3.3.2.4. Total Protein-Ligand Contacts

A timeline representation of the interactions and contacts (H-bonds, Hydrophobic, Ionic, and Water bridges) is summarized in the **Figure 9**. The top panel shows the total number of specific interactions the protein AChE makes with the ligand **10a** over the 100ns molecular dynamic simulation trajectory. The bottom panel shows which residues interact with the ligand in each

trajectory frame. Some residues, specifically: Tyr341, Phe338, Tyr337, Tyr124, and Trp86, make more than one specific interaction with the ligand **10a**, which is represented by a darker orange shade, according to the scale to the right of the plot.

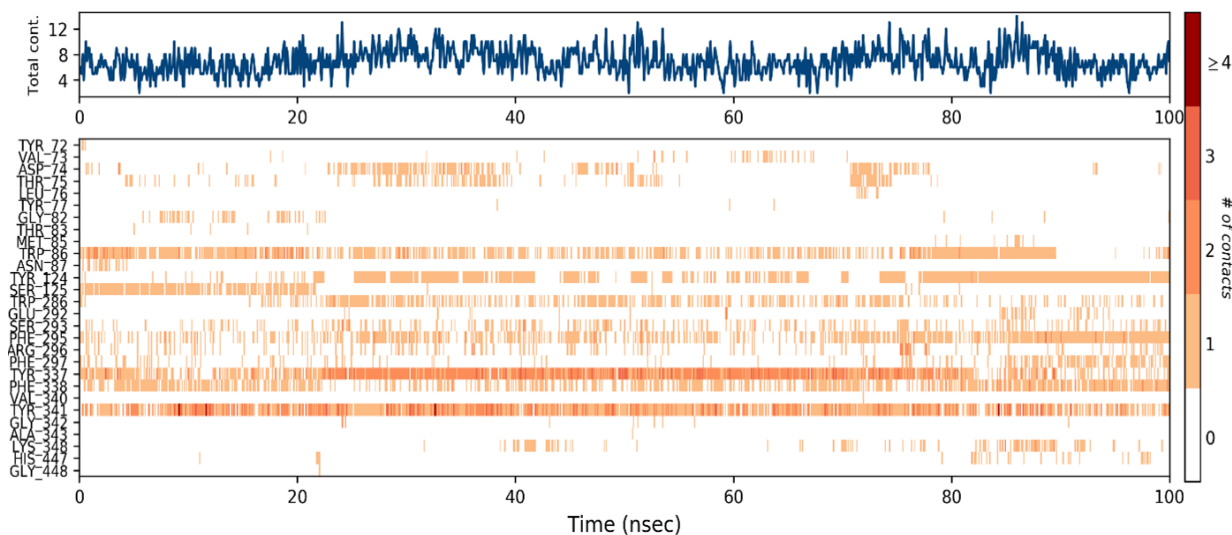


Figure 9. Total Protein-Ligand Contacts obtained from the molecular dynamic simulation trajectories.

3.3.2.5. Secondary structural analysis during simulation

An outstretched study has been carried out to comprehend the structural evolution of the AChE-ligand during the 100ns simulation. The way that the ligand adheres to the inhibition site of AChE is crucial in understanding the ligands' stability. To highlight this, four snapshots of the AChE-ligand complexes have been taken at every 25ns interval (25ns, 50ns, 75ns, and 100ns). It is observed that the secondary structure elements (helix and beta-sheets) remained conserved throughout the simulation process which highlights the stability and reliability of the AChE after binding to the ligands. A bit of fluctuation is observed in the N-terminal and the C-terminal coils, but structurally, no significant changes have been seen. It has also been observed that the ligands are constantly attached to the inhibition site without any structural modification, which implies that the ligand is highly stable. The Secondary structural analysis has shown no significant level of overall conformational change in ligand-bound to the AChE (**Figure 10**).

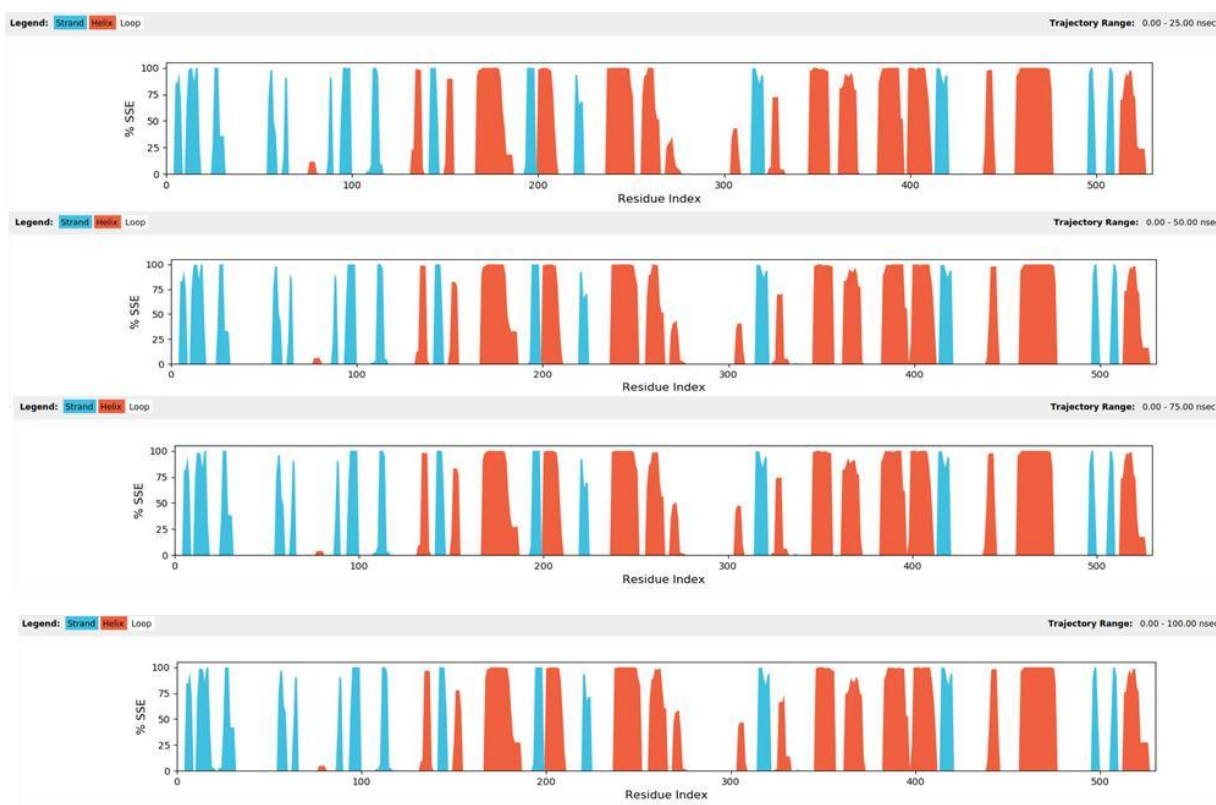


Figure 10. The secondary structure content of the AChE protein with the inhibitor **10a** during the molecular dynamic simulation.

Conclusion

In summary, twelve cyclosulfamide derivatives were synthesized and tested for their ability to inhibit AChE and BuChE against AD. The biological activity assay confirms that among 12 synthesized compounds; six are active against AChE enzyme and eight compounds are active against BuChE enzyme. Compound **10a** was found to be the best AChE inhibitor ($IC_{50}=45.30\pm 0.88\mu M$). Although compound **4a** demonstrated to be the most effective BuChE inhibitor ($IC_{50}=52.87\pm 3.73\mu M$).

The results of the molecular docking study of synthesized derivatives into the active site of AChE enzyme showed that **10a**, **11a**, and **5a** derivatives have a better docking score when compared with the reference ligand. The results established the utility of **10a**, **11a**, and **5a** molecules as suitable candidates for the inhibition of AChE enzyme. The obtained results from molecular docking investigation motivate us to confirm the predicted binding mode of compound **10a** using molecular dynamics simulation. Compound **10a** retained the same binding site after the MD simulation at 100 ns and the same hydrogen bonds, the hydrophobic interactions with the residues, are also retained.

Acknowledgements

This work was supported financially by The General Directorate for Scientific Research and Technological Development (DG-RSDT), Algerian Ministry of Scientific Research, Applied Organic Chemistry Laboratory (FNR 2000).

Disclosure statement

All authors declare no conflict of interest.

Funding

This research did not receive any specific grant from funding agencies in the public, commercial, or not-for-profit sectors.

ORCID

Abdeslem Bouzina <https://orcid.org/0000-0002-8908-8912>

Abdelhak Djemel <https://orcid.org/0000-0001-6442-4687>.

Omar Sekiou <https://orcid.org/0000-0003-2727-0740>.

Imededdine Kadi <https://orcid.org/0000-0002-4703-5783>.

Yousra Ouafa Bouone <https://orcid.org/0000-0002-3202-5304>.

Rachida Mansouri <https://orcid.org/0000-0002-6886-9269>.

Zineb Aouf <https://orcid.org/0000-0002-3873-8647>.

Nour Eddine Aouf <https://orcid.org/0000-0001-6819-708X>.

Références

[1] N. Lolak, M. Boga, M. Tuneg, G. Karakoc, S. Akocak, C.T. Supuran, Sulphonamides incorporating 1,3,5-triazine structural motifs show antioxidant, acetylcholinesterase, butyrylcholinesterase, and tyrosinase inhibitory profile, *J. Enzyme Inhib. Med. Chem.* 35 (2020) 424-431. <https://doi.org/10.1080/14756366.2019.1707196>.

[2] A. Akıncıoğlu, H. Akıncıoğlu, İ. Gülçin, S. Durdagi, C.T. Supuran, S. Göksu, Discovery of potent carbonic anhydrase and acetylcholine esterase inhibitors: Novel sulfamoylcarbarnates and sulfamides derived from acetophenones, *Bioorg. Med. Chem.* 23 (2015) 3592-3602. <https://doi.org/10.1016/j.bmc.2015.04.019>.

[3] M.J. Uddin, D. Russo, M.M. Rahman, S.B. Uddin, M.A. Halim, C. Zidorn, L. Milella, Anticholinesterase activity of eight medicinal plant species: in vitro and in silico studies in the search for therapeutic agents against Alzheimer's disease, *Evid. Based Complementary Altern. Med.* 2021 (2021) ID:9995614. <https://doi.org/10.1155/2021/9995614>.

- [4] P. Taslimi, M. Işık, F. Türkan, M. Durgun, C. Türkeş, İ. Gülçin, Ş. Beydemir, Benzenesulfonamide derivatives as potent acetylcholinesterase, α -glycosidase, and glutathione S-transferase inhibitors: biological evaluation and molecular docking studies, *J. Biomol. Struct. Dyn.* 39 (2021) 5449-5460. <https://doi.org/10.1080/07391102.2020.1790422>.
- [5] H. Göçer, A. Akıncioğlu, S. Göksu, İ. Gülçin, C.T. Supuran, Carbonic anhydrase and acetylcholinesterase inhibitory effects of carbamates and sulfamoylcarbamates, *J. Enzyme Inhib. Med. Chem.* 30 (2014) 316-320. <https://doi.org/10.3109/14756366.2014.928704>.
- [6] A. Akıncioğlu, M. Topal, İ. Gülçin, S. Göksu, Novel sulphamides and sulphonamides incorporating the tetralin scaffold as carbonic anhydrase and acetylcholine esterase inhibitors, *Arch. Pharm.* 347 (2013) 68-76. <https://doi.org/10.1002/ardp.201300273>.
- [7] M.M. Heravi, V. Zadsirjan, Prescribed drugs containing nitrogen heterocycles: an overview, *RSC adv.* 10 (2020) 44247-44311. <https://doi.org/10.1039/D0RA09198G>.
- [8] (a) S. Chhabra, K. Shah, The novel scaffold 1,2,4-benzothiadiazine-1,1-dioxide: a review, *Med Chem Res.* 30 (2021) 15-30. <https://doi.org/10.1007/s00044-020-02644-y>. (b) T. Abbaz, A. Bendjeddou, A. Gouasmia, D. Bouchouk, C. Boualleg, N. Kaouachi, N. Inguibert, D. Villemin, Synthesis, characterization and antibacterial activity of cyclic sulfamide linked to tetrathiafulvalene (TTF), *Lett. Org. Chem.* 11 (2014) 59-63. <https://doi.org/10.2174/157017861101140113162502>. (c) Z. Aouf, S. Bouacida, C. Benzaid, A. Amira, H. K'Tir, M. Mathé-allainmat, J. Lebreton, N-E. Aouf, Cyclic N-2-chloroethyl-sulfamide compounds with a phosphonate moiety: synthesis, characterization, x-ray crystallographic study and antimicrobial evaluation, *ChemistrySelect.* 6 (2021) 9722-9727. <https://doi.org/10.1002/slct.202102650>. (d) C. Başkan, A.G. Ertürk, B. Aydın, B. Sırıken, 3-Imino derivative-sulfahydantoin: Synthesis, in vitro antibacterial and cytotoxic activities and their DNA interactions, *Bioorg. Chem.* 119 (2022) 105517. <https://doi.org/10.1016/j.bioorg.2021.105517>.
- [9] D. Dou, K-C. Tiew, G. He, S.R. Mandadapu, S. Aravapalli, K.R. Alliston, Y. Kim, K-O. Chang, W.C. Groutas, Potent Inhibition of Norwalk Virus by Cyclic Sulfamide Derivatives, *Bioorg. Med. Chem.* 19 (2011) 5975-5983. <https://doi.org/10.1016/j.bmc.2011.08.054>.
- [10] J.J. Jun, D. Duscharla, R. Ummanni, P.R. Hanson, S.V. Malhotra, Investigation on the anticancer activity of symmetric and unsymmetric cyclic sulfamides, *ACS Med. Chem. Lett.* 12 (2021) 202-210. <https://doi.org/10.1021/acsmchemlett.0c00460>.

[11] J.Y. Winum, A. Scozzafava, J.L. Montero, C.T. Supuran, Therapeutic potential of sulfamides as enzyme inhibitors, *Med. Res. Rev.* 26 (2006) 767-792. <https://doi.org/10.1002/med.20068>.

[12] J.H. Lee, J.H. Bok, S.B. Park, H.S. Pagire, Y.J. Na, E. Rim, W.H. Jung, J.S. Song, N.S. Kang, H.W. Seo, K.Y. Jung, B.H. Lee, K.Y. Kim, J.H. Ahn, Optimization of cyclic sulfamide derivatives as 11β -hydroxysteroid dehydrogenase 1 inhibitors for the potential treatment of ischemic brain injury, *Bioorg Med Chem Lett.* 30 (2020) 126787. <https://doi:10.1016/j.bmcl.2019.126787>.

[13] A. Ax, W. Schaal, L. Vrang, B. Samuelsson, A. Hallberg, A. Karlén, Cyclic sulfamide HIV-1 protease inhibitors, with sidechains spanning from P2/P2' to P1/P1', *Bioorg Med Chem.* 13 (2005) 755-764. <https://doi.org/10.1016/j.bmc.2004.10.042>.

[14] T. Sparey, D. Beher, J. Best, M. Biba, J.L. Castro, E. Clarke, J. Hannam, T. Harrison, H. Lewis, Cyclic sulfamide gamma-secretase inhibitors, *Bioorg. Med. Chem. Lett.* 15 (2005) 4212-4216. <https://doi.org/10.1016/j.bmcl.2005.06.084>.

[15] S. Mekala, G. Nelson, Y.M. Li, Recent developments of small molecule γ -secretase modulators for Alzheimer's disease, *RSC Med Chem.* 11 (2020) 1003-1022. <https://doi.org/10.1039/d0md00196a>.

[16] L. Marinaccio, A. Stefanucci, G. Scioli, A. Della Valle, G. Zengin, A. Cichelli, A. Mollica, Peptide Human Neutrophil Elastase Inhibitors from Natural Sources: An Overview, *Int. J. Mol. Sci.* 23 (2022) 2924. <https://doi.org/10.3390/ijms23062924>.

[17] E. Black, J. Breed, A.L. Breeze, K. Embrey, R. Garcia, T.W. Gero, L. Godfrey, P.W. Kenny, A.D. Morley, C.A. Minshull, A.D. Pannifer, J. Read, A. Rees, D.J. Russell, D. Toader, J. Tucker, Structure-based design of protein tyrosine phosphatase-1B inhibitors, *Bioorg. Med. Chem. Lett.* 15 (2005) 2503-2507. <https://doi.org/10.1016/j.bmcl.2005.03.068>.

[18] T. Liu, B. Huang, Y. Tian, X. Liang, H. Liu, H. Liu, P. Zhan, E. De Clercq, C. Pannecouque, X. Liu, Design, synthesis, and biological evaluation of novel 4-aminopiperidinyl-linked 3,5-disubstituted-1,2,6-thiadiazine-1,1-dione derivatives as HIV-1 NNRTIs, *Chem. Biol. Drug. Des.* 86 (2015) 107-113. <https://doi.org/10.1111/cbdd.12468>.

[19] J. Liu, P.P. Shao, D. Guiadeen, A. Krikorian, W. Sun, Q. Deng, A-M. Cumiskey, R.A. Duffy, B.A. Murphy, K. Mitra, D.G. Johns, J.L. Duffy, P. Vachal, Cholesteryl ester transfer

protein (CETP) inhibitors based on cyclic urea, bicyclic urea and bicyclic sulfamide cores, *Bioorg. Med. Chem. Lett.* 32 (2021) 127668. <https://doi.org/10.1016/j.bmcl.2020.127668>.

[20] D. Dou, S.R. Mandadapu, K.R. Alliston, Y. Kim, K-O. Chang, W.C. Groutas, Cyclosulfamide-based derivatives as inhibitors of noroviruses, *Eur. J. Med. Chem.* 47 (2012) 59-64. <https://doi.org/10.1016/j.ejmech.2011.10.019>.

[21] G.L. Ellman, K.D. Courtney, V. Andres, R.M. Featherstone, A new and rapid colorimetric determination of acetylcholinesterase activity, *Biochem. Pharmacol.* 7 (1961) 88-95. [https://doi.org/10.1016/0006-2952\(61\)90145-9](https://doi.org/10.1016/0006-2952(61)90145-9).

[22] J. Cheung, M.J. Rudolph, F. Burshteyn, M.S. Cassidy, E.N. Gary, J. Love, M.C. Franklin, J.J. Height, Structures of human acetylcholinesterase in complex with pharmacologically important ligands, *J. Med. Chem.* 55 (2012) 10282-10286. <https://doi.org/10.1021/jm300871x>.

[23] S. Release (2015). 2 (2015) LigPrep, version 3.4. Schrödinger, LLC, New York, NY, 26400175.

[24] R.A. Friesner, J. L. Banks, R.B. Murphy, T.A. Halgren, J.J. Klicic, D.T. Mainz, M.P. Repasky, E.H. Knoll, D.E. Shaw, M. Shelley, J.K. Perry, P. Francis, P.S. Shenkin, Glide: A new approach for rapid, accurate docking and scoring. 1. method and assessment of docking accuracy, *J. Med. Chem.* 47 (2004). 1739–1749. <https://doi.org/10.1021/jm0306430>.

[25] R.A. Friesner, R.B. Murphy, M.P. Repasky, L.L. Frye, J.R. Greenwood, T.A. Halgren, D.T. Mainz, Extra precision glide: Docking and scoring incorporating a model of hydrophobic enclosure for protein-ligand complexes. *J. Med. Chem.* 49 (2006) 6177–6196. <https://doi.org/10.1021/jm051256o>.

[26] E.F. Pettersen, T.D. Goddard, C.C. Huang, G.S. Couch, D.M. Greenblatt, E.C. Meng, T.E. Ferrin, UCSF Chimera--a visualization system for exploratory research and analysis, *J. Comput. Chem.* 25 (2004) 1605-1612. <https://doi.org/10.1002/jcc.20084>.

[27] (a) L.L.C. Schrödinger, (2015) Schrödinger Release 2015-4: Desmond molecular dynamics system, Maestro-Desmond interoperability tools, DE Shaw Research. Schrödinger, New York, NY. (b) E. Chow, C.A. Rendleman, J.K. Bowers, R.O. Dror, D.H. Hughes, J. Gullingsrud, F.D. Sacerdoti, D.E. Shaw, Desmond performance on a cluster of multicore processors, (2008) DE Shaw Research Technical Report DESRES/TR-2008-01.

[28] (a) A. Bouzina, K. Bechlem, H. Berredjem, B. Belhani, I. Becheker, J. Lebreton, M. Le Borgne, Z. Bouaziz, C. Marminon, M. Berredjem, Synthesis, spectroscopic characterization,

and in vitro antibacterial evaluation of novel functionalized sulfamidocarbonyloxyphosphonates. *Molecules*, 23 (2018) 1682.

<https://doi.org/10.3390/molecules23071682>. (b) A. Bouzina, M. Berredjem, A. Nocentini, S. Bua, Z. Bouaziz, J. Jose, M. Le Borgne, C. Marminon, P. Gratteri, C.T. Supuran, Ninhydrins inhibit carbonic anhydrases directly binding to the metal ion, *Eur. J. Med. Chem.* 209 (2021) 112875. <https://doi.org/10.1016/j.ejmech.2020.112875>.

[29] (a) A. Bouzina, N-E. Aouf, M. Berredjem, Ultrasound assisted green synthesis of α -hydroxyphosphonates under solvent-free conditions, *Res. Chem. Intermed.* 42 (2016) 5993-6002. <https://doi.org/10.1007/s11164-015-2420-8>. (b) R. Redjemia, A. Bouzina, Y.O. Bouone, A. Mansouri, R. Bahadi, M. Berredjem, Copper (I) bromide (CuBr): a highly efficient catalyst for the synthesis of β -enaminone derivatives using ultrasound irradiation under solvent-free conditions, *Res. Chem. Intermed.* 48 (2022) 4947-4962. <https://doi.org/10.1007/s11164-022-04853-z>. (c) A. Amira, Z. Aouf, H. K'tir, Y. Chemam, R. Ghodbane, R. Zerrouki, N-E. Aouf, Recent advances in the synthesis of α -aminophosphonates: A Review, *ChemistrySelect* 6 (2021) 6137-6149. <https://doi.org/10.1002/slct.202101360>.

[30] A. Bouzina, M. Berredjem, B. Belhani, S. Bouacida, C. Marminon, M. Le Borgne, Z. Bouaziz, M. Aissaoui, Microwave-accelerated multicomponent synthesis and X-ray characterization of novel benzothiadiazinone dioxide derivatives, analogues of Monastrol, *Res. Chem. Intermed.* 47 (2021) 1359-1376. <https://doi.org/10.1007/s11164-020-04378-3>.

[31] A. Skrzypek, J. Matysiak, M.M. Karpińska, A. Niewiadomy, Synthesis and anticholinesterase activities of novel 1,3,4-thiadiazole based compounds, *J. Enz. Inhib. Med. Chem.* 28 (2012) 816–823. <https://doi.org/10.3109/14756366.2012.688041>.

[32] B. Zhou, H. Li, Z. Cui, D. Li, H. Geng, J. Gao, L. Zhou, Simple analogues of natural product chelerythrine: Discovery of a novel anticholinesterase 2-phenylisoquinolin-2-ium scaffold with excellent potency against acetylcholinesterase, *Eur. J. Med. Chem.* (2020) 112415. <https://doi.org/10.1016/j.ejmech.2020.112415>.

[33] S. Omidpanah, Y. Vahedi-Mazdabadi, A. Manayi, A. Rastegari, R. Hariri, E. Mortazavi-Ardestani, M. Eftekhari, M. Khanavi, T. Akbarzadeh, M. Saeedi, Phytochemical investigation and anticholinesterase activity of ethyl acetate fraction of *Myristica fragrans* Houtt. seeds, *Nat. Prod. Res.* 36 (2020) 610-616. <https://doi.org/10.1080/14786419.2020.1788555>.

[34] N. Lolak, S. Akocak, C. Türkeş, P. Taslimi, M. Işık, Ş. Beydemir, İ. Gülçin, M. Durgun, Synthesis, characterization, inhibition effects, and molecular docking studies as acetylcholinesterase, α -glycosidase, and carbonic anhydrase inhibitors of novel

benzenesulfonamides incorporating 1,3,5-triazine structural motifs, *Bioorg. Chem.* 100 (2020) 103897. <https://doi.org/10.1016/j.bioorg.2020.103897>.

[35] Q. Yang, Y. Li, D. Dou, X. Gan, S. Mohan, C.S. Groutas, L.E. Stevenson, Z. Lai, K.R. Alliston, J. Zhong, T.D. Williams, W.C. Groutas, Inhibition of serine proteases by a new class of cyclosulfamide-based carbamylating agents, *Arch. Biochem. Biophys.* 475 (2008) 115–120. <https://doi.org/10.1016/j.abb.2008.04.020>.

[36] Z. Lai, X. Gan, L. Wei, K.R. Alliston, H. Yu, Y.H. Li, W.C. Groutas, Potent inhibition of human leukocyte elastase by 1,2,5-thiadiazolidin-3-one 1,1 dioxido-based sulfonamide derivatives, *Arch. Biochem. Biophys.* 429 (2004) 191–197. <https://doi.org/10.1016/j.abb.2004.06.014>.

[37] F. Mehrabi, Y. Pourshojaei, A. Moradi, M. Sharifzadeh, L. Khosravani, R. Sabourian, A. Foroumadi, Design, synthesis, molecular modeling and anticholinesterase activity of benzylidene-benzofuran-3-ones containing cyclic amine side chain, *Future Med. Chem.* 9 (2017) 659–671. <https://doi.org/10.4155/fmc-2016-0237>.

[38] I. Boualia, C. Derabli, R. Boulcina, C. Bensouici, M. Yildirim, A. Birinci Yildirim, A. Debache, Synthesis, molecular docking studies, and biological evaluation of novel alkyl bis(4-amino-5-cyanopyrimidine) derivatives, *Arch. Pharma.* 352 (2019) 1900027. <https://doi.org/10.1002/ardp.201900027>.

[39] S. Burmaoglu, A.O. Yilmaz, M.F. Polat, R. Kaya, İ. Gulcin, O. Algul, Synthesis of novel tris-chalcones and determination of their inhibition profiles against some metabolic enzymes, *Arch. Physiol. Biochem.* 127 (2019) 153–161. <https://doi.org/10.1080/13813455.2019.1623265>.

[40] I. Kufareva, R. Abagyan, Methods of protein structure comparison, *Methods Mol. Biol.* 857 (2012) 231–257. https://doi.org/10.1007/978-1-61779-588-6_10.

[41] M.A. Langarizadeh, K. Eskandari, A. Abiri, M.R. Tavakoli, A. Asadipour, Y. Pourshojaei, A novel dual three and five-component reactions between dimedone, aryl aldehydes, and 1-naphthylamine: synthesis and computational studies, *J. Mol. Struct.* 1258 (2022) 132569. <https://doi.org/10.1016/j.molstruc.2022.132569>.

[42] M.Z. Hernandez, S.M.T. Cavalcanti, D.R.M. Moreira, W.F. de Azevedo Junior, A.C.L. Leite, Halogen atoms in the modern medicinal chemistry: hints for the drug design, *Curr. Drug Targets*, 11 (2010) 303–314. <https://doi.org/10.2174/138945010790711996>.